INTERNATIONAL JOURNAL FOR NUMERICAL METHODS IN FLUIDS, VOL. 23, 503–524 (1996)

BEM SOLUTION FOR THE PROBLEM OF FLUX OF A MULTICOMPONENT MIXTURE OF GASES OUT OF A MULTILAYER LANDFILL

V. POPOV* AND H. POWER†

Wessex Institute of Technology, Southampton SO40 7AA, U.K.

SUMMARY

A two-dimensional numerical model for convection–diffusion flow of a multigas mixture through a multilayer porous medium was developed with the aim to be used for evaluation of emissions of gases from landfills. The proposed model is based on the boundary element–dual reciprocity method. Time-independent one-dimensional analytical solutions for a multilayer domain were found for the cases of a single gas and a two-gas mixture and used to verify the accuracy of the model. Although the proposed technique is a simple one, consisting only of boundary integrals, it was found that the technique can be applied with satisfactory accuracy to the problem at which it was initially aimed.

KEY WORDS: flow of gases; porous media; landfill; BEM numerical simulation

1. INTRODUCTION

One of the most popular ways to dispose of domestic and industrial waste is to bury it under layers of soil, usually called landfill. A major concern derived from this disposal of waste is the generation of gases, mainly carbon dioxide (CO_2) and methane (CH_4), due to the degradation of waste materials in the repository. CO_2 and CH_4 are powerful infrared absorber gases. The presence of these gases in the atmosphere traps heat between the surface of the earth and the upper atmosphere. Therefore an increase in such gases can cause an increase in the earth's temperature, an effect that is commonly referred to as the greenhouse effect.

The primary source of gas production is the anaerobic microbial degradation of organic materials such as food waste, garden waste, paper, textiles, resins, bitumen, etc. This process begins after the waste has been in the landfill for 10–50 days. Although the majority of CH_4 and CO_2 is generated within 20 years of landfill completion, emissions can continue for 100 years or more.

Of the various gas byproducts, methane is the one of primary concern. Methane is produced by the action of micro-organisms on the degradable waste. The complex organic molecules in the above substances are broken down to smaller molecules. The process of forming methane is a two-stage one. First the large organic molecules are broken down by hydrolysis to smaller, more soluble

* On leave from Center for Application of Radioisotopes, Skopje, Macedonia.
† Corresponding author. On leave from Instituto de Mecánica de Fluídos, Universidad Central de Venezuela, Caracas, Venezuela.

CCC 0271–2091/96/050503–22

Received June 1995
Revised January 1996

compounds. These include simple sugars, amino acids, fatty acids and alcohols. This stage is known as 'acidification'. The next stage involves further hydrolysis of the primary products to fatty acids. These are then metabolized by bacteria to produce methane. Landfills are estimated to be the major source of CH_4 emissions and account for about 38 per cent of total anthropogenic sources.

Pressurization of the repository due to the internal gas production induces the emission of methane into the atmosphere. Methane (CH_4) is an important greenhouse gas. It plays a major role in controlling the abundance of both tropospheric ozone (O_3), which is an important greenhouse gas near the tropopause, and the hydroxyl (OH) radical, which controls the atmospheric lifetimes of other gases of climate importance.[1–3] Methane can also be oxidized to form CO_2.

In 1991 the atmospheric concentration of CH_4 was about 1·72 ppmv, which is more than double the pre-industrial level of about 0·8 ppmv.[1] The current annual rate of accumulation is about 13 ppbv or 37 Mt, which is lower than the annual rate of 20 ppbv observed in the late 1970s.[1,4]

The main objective of this work is to develop a 2D numerical model, based on the boundary element method (BEM), to solve the problem of the flux of a multicomponent mixture of gases out of a multilayer landfill. The boundary element method is now a well-established numerical technique for the analysis of engineering problems (for more details see Reference 5). One of its main advantages is the considerable reduction in data preparation in relation to domain methods, since only surface elements are necessary, as well as its versatility in dealing with subdomain matching, which is of crucial importance in the present problem. The basis of the method is that a fundamental solution is used to take some of or all the terms in the governing equation to the boundary.

2. GOVERNING EQUATION

The governing equation for the two-dimensional flow of a mixture of N compressible gases through a multilayer (M-layer) porous medium, when each layer is isotropic and homogeneous, is usually described by the following system of $N \times M$ equations (see e.g. References 6 and 7):

$$\sum_{l=1}^{2}\left[\frac{\partial}{\partial x_l}\left(D_i^j \frac{\partial c_i}{\partial x_l}\right)\right] - \sum_{l=1}^{2}\frac{\partial (c_i V_l^j)}{\partial x_l} + P_i^j - d_i^j c_i - n^j \frac{\partial c_i}{\partial t} = 0 \qquad (i = 1, \ldots, N, \quad j = 1, \ldots, M), \tag{1}$$

where

c_i gas concentration of ith gas (kg m^{-3})
D_i^j diffusion coefficient of ith gas in jth layer (m^2 s^{-1})
V_l^j velocity of mixture of gases in lth direction in jth layer (m s^{-1})
P_i^j production term for ith gas in jth layer (kg m^{-3} s^{-1})
d_i^j reaction constant for ith gas in jth layer (s^{-1})
n^j material porosity of jth layer (%)
x_l lth co-ordinate (m)
t time (s).

Formally the above equation is valid for a binary mixture, with D_i^j constant, and for a multicomponent mixture of N gases, with $N > 2$, when $N - 1$ of them behave as dilute components diffusing in a homogeneous mixture, which is considered as the carrying fluid (air in our case, initially trapped in the porous medium, which we will consider as only N_2 with initial concentration 0·7 kg m^{-3}). The diffusion coefficient of the dilute components in the multigas mixture is a function of the concentrations of each of the gases in the mixture. When the binary diffusion coefficients

between one component and each of the other components of the mixture are approximately the same, it is found that to a first approximation the diffusion coefficients in (1) are independent of the concentrations (for more details see Reference 8). Here for simplicity we will restrict ourself to the case of constant diffusion coefficients, although they can change from layer to layer.

The diffusion coefficient D for a porous medium differs from the diffusion coefficient D_0 for a standard medium, usually a gas without any solid or liquid present. It is known that the pore structure influences the diffusion regime. Imagine a porous medium under uniform pressure containing a multicomponent gas mixture. When the pore diameter is large enough for molecular diffusion to prevail, the diffusion flux will be independent of the pore diameter. However, as the pore diameter decreases, the resistance due to molecular–soil particle collisions appears and the flux tends to decrease. The complex geometries of porous materials make it necessary to use equations that empirically relate the variable D/D_0 to porous structure parameters.

The most frequently used equations are

$$D/D_0 = a(n - b) \tag{2}$$

and

$$D/D_0 = An^B, \tag{3}$$

where n represents porosity, while a and b or A and B are determined by fitting curves to experimental data. Tables containing values of the parameters a and b or A and B can be found in Reference 7. The velocity vector is given by Darcy's law as the gradient of the total pressure of the mixture of gases,

$$V_l^j = -\frac{k^j}{\mu}\frac{\partial p}{\partial x_l}, \tag{4}$$

where

p total pressure of gases (N m^{-2})
k^j intrinsic permeability for jth layer (m^2)
μ dynamic viscosity of mixture of gases (N s m^{-2})

As in the case of the diffusion coefficient D_i^j, the dynamic viscosity μ is also a function of the concentrations of each of the gases in the mixture, which for the above case of a dilute mixture can be considered as a constant.

The gas pressure function is given by

$$p = \sum_{i=1}^{N} a_i c_i^{d_i}, \tag{5}$$

where

a_i R_iT
R_i gas constant of ith gas (J K^{-1} kg^{-1})
T absolute temperature (K).

The exponent determines the curvature of the gas pressure function. For $d_i = 1$ the gas pressure function reduces to the ideal gas equation, which is generally the case under landfill conditions.

Substitution of (4) and (5) into (1) leads to the non-linear partial differential equation system

$$D_i^j \sum_{l=1}^{2} \frac{\partial^2 c_i}{\partial x_l^2} + \sum_{l=1}^{2} \frac{\partial}{\partial x_l}\left[c_i\left(\sum_{m=1}^{N} K_m^j \frac{\partial c_m}{\partial x_l}\right)\right] + P_i^j - d_i^j c_i - n^j \frac{\partial c_i}{\partial t} = 0 \quad (i = 1, \ldots, N, \quad j = 1, \ldots, M), \tag{6}$$

where

$$K_m^j = \frac{k^j}{\mu} a_m = \frac{k^j}{\mu} R_m T \quad (\mathrm{m^5\ kg^{-1}\ s^{-1}}).$$

The flux of the ith gas in the direction of the normal n on the boundary of the jth layer is given by

$$\Phi_i^j = -D_i^j \frac{\partial c_i}{\partial n} - c_i\left[\sum_{k=1}^{N}\left(K_k^i \frac{\partial c_k}{\partial n}\right)\right] \quad (i = 1, \ldots, N, \quad j = 1, \ldots, M), \tag{7}$$

where the normal vector is defined outwardly to each layer.

The following boundary and initial conditions have to be satisfied: on the impermeable surfaces,

$$\frac{\partial c_i}{\partial n} = 0;$$

on the free surface,

$$c_i = C_{i0} \quad \text{or} \quad c_i = 0,$$

according to whether the gas under consideration is initially on the repository or not; and at $t = 0$, $C_i = C_{i0}$ or $c_i = 0$ inside the fluid domain, according to the above free surface condition.

The above boundary conditions as well as the geometry of the multilayer domain are shown in Figure 1.

At each interface the flux leaving one layer has to be equal to the flux entering the next layer for each of the gases. Therefore it is necessary that the following matching conditions hold at the mth interface between layers:

$$\left\{-D_i^m \frac{\partial c_i^m}{\partial n} - c_i^m\left[\sum_{k=1}^{N}\left(K_k^m \frac{\partial c_k^m}{\partial n}\right)\right]\right\}\Big|_m = \left\{-D_i^{m+1} \frac{\partial c_i^{m+1}}{\partial n} - c_i^{m+1}\left[\sum_{k=1}^{N}\left(K_k^{m+1} \frac{\partial c_k^{m+1}}{\partial n}\right)\right]\right\}\Big|_m \tag{8}$$
$$(i = 1, \ldots, N, \quad m = 1, \ldots, M-1).$$

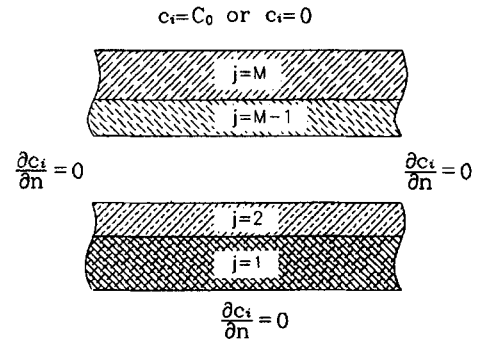

Figure 1. Boundary conditions and geometry of multilayer domain

In addition to the above conditions, the concentration needs to be continuous at each interface, i.e.

$$c_i^m|_m = c_i^{m+1}|_m \quad (i = 1, \ldots, N, \quad m = 1, \ldots, M-1). \tag{9}$$

The $2N(M-1)$ matching conditions (equations (8) and (9)) together with the $N \times M$ equations for the concentration on each layer and the boundary and initial conditions complete the formulation of the problem.

When the constants K_i^j, D_i^j and d_i^j are the same for all gases in each layer, i.e. equal to K^j, D^j and d^j, the addition of all N equations (6) yields a single equation for the mixture of gases in a multilayer domain (single-gas equation),

$$D^j \sum_{l=1}^{2} \frac{\partial^2 c}{\partial x_l^2} + \sum_{l=1}^{2} \frac{\partial}{\partial x_l}\left(cK^j \frac{\partial c}{\partial x_l}\right) + P^j - d^j c - n^j \frac{\partial c}{\partial t} = 0 \quad (j = 1, \ldots, M), \tag{10}$$

where

$$P^j = \sum_{i=1}^{N} P_i^j, \qquad c = \sum_{i=1}^{N} c_i.$$

The flux of the mixture of gases in the direction of the normal n on the boundary of the jth layer is given by

$$\Phi^j = -(D^j + cK^j)\frac{\partial c}{\partial n} \quad (j = 1, \ldots, M). \tag{11}$$

The matching conditions at each interface now become

$$-(D^m + cK^m)\frac{\partial c^m}{\partial n}\bigg|_m = -(D^{m+1} + cK^{m+1})\frac{\partial c^{m+1}}{\partial n}\bigg|_m \quad (m = 1, \ldots, M-1), \tag{12}$$

while the continuity equation becomes

$$c^m|_m = c^{m+1}|_m \quad (m = 1, \ldots, M-1). \tag{13}$$

The following boundary and initial conditions have to be satisfied: on the impermeable surfaces,

$$\frac{\partial c}{\partial n} = 0;$$

and on the free surface,

$$c = C_0 = \sum_{i=1}^{N} C_{i0}.$$

3. BOUNDARY ELEMENT FORMULATION

The main difficulty in applying the BEM to the above non-linear system of partial differential equations is the lack of a fundamental solution for non-linear equations. Thus it is necessary to rewrite the partial differential equations in terms of a linear operator (with a known fundamental solution), with the non-linear terms appearing as non-homogeneous terms (pseudobody forces). In this way, starting from the integral representation formula for the linear operator, an integral equation can be found where the non-linear terms generate domain integrals. In early boundary element analysis the evaluation of domain integrals was done using cell integration, a technique which, whilst effective and general, made the method lose its boundary-only nature, introducing an additional internal discretization.

Several methods have been developed to take domain integrals to the boundary in order to eliminate the need for internal cells. One of the most effective to date is the dual reciprocity method (DRM) introduced by Nardini and Brebbia.[9] This method is closely related to the method of particular integrals introduced by Ahmad and Banerjee,[10] which is also used to transform domain integrals to boundary integrals. In the latter method a particular solution satisfying the non-homogeneous partial differential equation (PDE) is first found and then the remainder of the solution satisfying the corresponding homogeneous PDE is obtained by solving the corresponding integral equations. The boundary conditions for the homogeneous PDE must be adjusted to ensure that the total solution satisfies the boundary conditions of the original problem. The DRM also uses the concept of particular solutions, but instead of solving for the particular solution and the homogeneous solution separately, it applies the divergence theorem to the domain integral terms and converts the domain integrals into equivalent boundary integrals. For the case in which the non-homogeneous term is a known function, the method of particular integrals is numerically more efficient than the DRM, but for the case in which the non-homogeneous term is an unknown function, as is the present case, the two methods are numerically equivalent.

In order to apply the BEM to find the solution of the non-linear system of partial differential equations (6), we rewrite them in terms of the Laplacian linear operator, with the non-linear, the decay, the source and the non-permanent terms as non-homogeneous terms of the Laplacian operator:

$$(D_i^j + K_i^j c_i)\nabla^2 c_i + c_i\left(\sum_{m=1}^{N}(K_m^j \nabla^2 c_m)(1-\delta_{mi})\right) = R_i^j \quad (i=1,\ldots,N, \quad j=1,\ldots,M),$$

where

$$R_i^j = -\sum_{l=1}^{2}\left[\frac{\partial c_i}{\partial x_l}\left(\sum_{m=1}^{N} K_m^j \frac{\partial c_m}{\partial x_l}\right)\right] - P_i^j + d_i^j c_i + n^j \frac{\partial c_i}{\partial t} \tag{14}$$

and δ_{mi} is the Kronecker delta function.

From the above system we can obtain a non-homogeneous Laplace equation for each gas, where the non-homogeneous terms are functions of the concentrations of all the gases involved and their first derivatives, i.e.

$$\nabla^2 c_i = b_i^j \quad (i=1,\ldots,N, \quad j=1,\ldots,M), \tag{15}$$

where

$$\begin{aligned} b_i^j = &\left[\prod_{p=1}^{N} D_p^j + \sum_{m=1}^{N}\left(K_m^j c_m \prod_{p=1}^{N}[D_p^j(1-\delta_{mp})+\delta_{mp}]\right)\right]^{-1} \\ &\times\left\{R_i^j\left[\prod_{p=1}^{N}[D_p^j(1-\delta_{pi})+\delta_{pi}] + \sum_{m=1}^{N}\left((1-\delta_{mi})K_m^j c_m \prod_{p=1}^{N}\{[D_p^j(1-\delta_{ip})+\delta_{ip}](1-\delta_{mp})+\delta_{mp}\}\right)\right]\right. \\ &\left. - c_i \sum_{m=1}^{N}\left((1-\delta_{mi})K_m^j R_m^j \prod_{p=1}^{N}\{[D_p^j(1-\delta_{ip})+\delta_{ip}](1-\delta_{mp})+\delta_{mp}\}\right)\right\} \quad (j=1,\ldots,M). \end{aligned}$$

From the Green integral representation formula it is found that the gas concentration at a point x for the ith gas and jth layer is given by

$$\lambda(x)c_i(x) + \int_{\Gamma^j} q^*(x,y)c_i(y)\mathrm{d}\Gamma_y - \int_{\Gamma^j} c^*(x,y)q_i(y)\mathrm{d}\Gamma_y = \int_{\Omega^j} c^*(x,y)b_i^j(y)\mathrm{d}\Omega_y. \tag{16}$$

Here $c^*(x, y)$ is the fundamental solution of the Laplace equation, which for an isotropic two-dimensional medium is given by

$$c^*(x,y) = \frac{1}{2\pi}\log\left(\frac{1}{r}\right),$$

where r is the distance from the point of application of the concentrated unit source to any other point under consideration, i.e. $r = |x - y|$, $q_i(y) = \partial c_i(y)/\partial n$ and $q^*(x, y) = \partial c^*(x, y)/\partial n$. Notice that in (16) all the integrals are over the boundary, with the exception of the one corresponding to the term $b_i(y)$. The constants $\lambda(x)$ have values between unity and zero, being equal to $\frac{1}{2}$ for smooth boundaries. It is also important to point out that the above equation holds for points inside the porous medium, in which case $\lambda(x) = 1$.

In the above equations we have written x instead of $\mathbf{x}$ and y instead of $\mathbf{y}$ and for convenience this notation will be used from here on.

In order to express the domain integral in (16) in terms of equivalent boundary integrals, a DRM approximation is introduced. The basic idea is to expand the term $b_i^j(y)$ using radial approximation functions, i.e.

$$b_i^j(y) = \sum_{k=1}^{J^j+I^j} f^j(y, z^k)\alpha_{ik}^j \quad (i = 1, \ldots, N, \quad j = 1, \ldots, M), \tag{17}$$

where $b_i^j(y)$ is the value of the function b_i^j at the point y. The functions $f^j(y, z^k)$ are approximating functions which depend only on the geometry of the problem, while the constants α_{ik}^j are unknown coefficients. The approximation is done at $J^j + I^j$ nodes, i.e. J^j boundary nodes and I^j internal nodes. Generally in the DRM approach the function $f^j(y, z^k)$ is chosen as

$$f^j(y, z^k) = 1 + R^j(y, z^k), \tag{18}$$

where $R^j(y, z^k)$ is the distance between a prespecified fixed collocation point z^k and a field point y where the function is approximated, i.e. $R^j(y, z^k) = |y - z^k|$.

The function (18) is a member of a family of functions known as radial basis functions, related to the theory of mathematical interpolation.

To obtain the coefficients α_{ik}^j in (17), we have to assume that the matrix generated by the evaluation of the function (18) at all the collocation points is non-singular. Michelli[11] has proved that when the nodal points are all distinct, the matrix resulting from a radial basis function is always non-singular.

With this approximation for the non-homogeneous term $b_i^j(y)$ the domain integral in (16) becomes

$$\int_{\Omega^j} c^*(x,y)b_i^j(y)\mathrm{d}\Omega_y = \sum_{k=1}^{J^j+I^j} \alpha_{ik}^j \int_{\Omega^j} c^*(x,y) f^j(y, z^k)\mathrm{d}\Omega_y \quad (i = 1, \ldots, N, \quad j = 1, \ldots, M). \tag{19}$$

To reduce the last domain integral in the above equation to equivalent boundary integrals, let us define a new auxiliary non-homogeneous Laplacian field $\hat{c}^j(y, z^k)$ for each collocation point z^k as

$$\nabla^2\hat{c}^j(y, z^k) = f^j(y, z^k), \tag{20}$$

whose particular solution for the 2D problem, when $f^j(y, z^k)$ is given by (18), is

$$\hat{c}^j(y, z^k) = \frac{(R^j(y, z^k))^2}{4} + \frac{(R^j(y, z^k))^3}{9}.$$

Applying the Green formula to the non-homogeneous Laplacian field $\hat{c}^j(x, z^k)$ at a point x, we obtain

$$\int_{\Omega^j} c^*(x, y) f^j(y, z^k) \mathrm{d}\Omega_y = \lambda(x)\hat{c}^j(x, z^k) + \int_{\Gamma^j} q^*(x, y)\hat{c}^j(y, z^k)\mathrm{d}\Gamma_y - \int_{\Gamma^j} c^*(x, y)\hat{q}^j(y, z^k)\mathrm{d}\Gamma_y.$$

Substituting the last equation into (19), the domain integral can be recast in the form

$$\int_{\Omega^j} c^*(x, y) b_i^j(y)\mathrm{d}\Omega_y = \sum_{k=1}^{J^j+I^j}\left[\alpha_{ik}^j\left(\lambda(x)\hat{c}^j(x, z^k) + \int_{\Gamma^j} q^*(x, y)\hat{c}^j(y, z^k)\mathrm{d}\Gamma_y - \int_{\Gamma^j} c^*(x, y)\hat{q}^j(y, z^k)\mathrm{d}\Gamma_y\right)\right].$$

Using the resulting expression in (16), one finally arrives at a boundary- only integral representation formula for the gas concentration,

$$\begin{aligned}\lambda(x)c_i(x) &+ \int_{\Gamma^j} q^*(x, y)c_i(y)\mathrm{d}\Gamma_y - \int_{\Gamma^j} c^*(x, y)q_i(y)\mathrm{d}\Gamma_y \\ &= \sum_{k=1}^{J^j+I^j}\left[\alpha_{ik}^j\left(\lambda(x)\hat{c}^j(x, z^k) + \int_{\Gamma^j} q^*(x, y)\hat{c}^j(y, z^k)\mathrm{d}\Gamma_y - \int_{\Gamma^j} c^*(x, y)\hat{q}^j(y, z^k)\mathrm{d}\Gamma_y\right)\right]. \qquad (21)\end{aligned}$$

For the numerical solution of the problem, equation (21) is written in a discretized form in which the boundary integrals are approximated by a summation of integrals over individual boundary elements, i.e.

$$\begin{aligned}\lambda(x)c_i(x) &+ \sum_{m=1}^{L^j}\int_{\Delta\Gamma_m^j} q^*(x, y)c_i(y)\mathrm{d}\Gamma_y - \sum_{m=1}^{L^j}\int_{\Delta\Gamma_m^j} c^*(x, y)q_i(y)\mathrm{d}\Gamma_y \\ &= \sum_{k=1}^{J^j+I^j}\left[\alpha_{ik}^j\left(\lambda(x)\hat{c}^j(x, z^k) + \sum_{m=1}^{L^j}\int_{\Delta\Gamma_m^j} q^*(x, y)\hat{c}^j(y, z^k)\mathrm{d}\Gamma_y - \sum_{m=1}^{L^j}\int_{\Delta\Gamma_m^j} c^*(x, y)\hat{q}^j(y, z^k)\mathrm{d}\Gamma_y\right)\right],\end{aligned}$$

which can be rewritten as

$$\begin{aligned}\lambda(x)c_i(x) &+ \sum_{m=1}^{L^j} H_m^j(x)c_{im} - \sum_{m=1}^{L^j} G_m^j(x)q_{im} \\ &= \sum_{k=1}^{J^j+I^j}\left[\alpha_{ik}^j\left(\lambda(x)\hat{c}^j(x, z^k) + \sum_{m=1}^{L^j} H_m^j(x)\hat{c}_{km}^j - \sum_{m=1}^{L^j} G_m^j(x)\hat{q}_{km}^j\right)\right] \qquad (22) \\ &\qquad (i = 1, \ldots, N, \quad j = 1, \ldots, M),\end{aligned}$$

where $H_m^j(x)$ and $G_m^j(x)$ are the resultants of integration over the boundary elements and L_j is the number of boundary elements in the jth layer. Equation (22) can be written in matrix form, which yields

$$\mathbf{H}^j\mathbf{c}_i - \mathbf{G}^j\mathbf{q}_i = (\mathbf{H}^j\hat{\mathbf{C}}^j - \mathbf{G}^j\hat{\mathbf{Q}}^j)\boldsymbol{\alpha}_i^j. \qquad (23)$$

The coefficients of α_i^j in the above equation can be calculated by evaluating equation (17) at all $J^j + I^j$ nodes, i.e.

$$\boldsymbol{\alpha}_i^j = (\mathbf{F}^j)^{-1}\mathbf{b}_i^j, \qquad (24)$$

and therefore its evaluation depends on the DRM approximation of each of the terms defining the non-homogeneous term b_i^j.

Substituting equation (24) into (23) yields

$$\mathbf{H}^j\mathbf{c}_i - \mathbf{G}^j\mathbf{q}_i = (\mathbf{H}^j\hat{\mathbf{C}}^j - \mathbf{G}^j\hat{\mathbf{Q}}^j)(\mathbf{F}^j)^{-1}\mathbf{b}_i^j. \tag{25}$$

To obtain the DRM approximation of the first derivative of the concentration, let us define the following approximation for the concentration,

$$\mathbf{c}_i = \mathbf{F}^j\boldsymbol{\beta}_i^j \quad (i = 1, \ldots, N, \quad j = 1, \ldots, M), \tag{26}$$

where $\boldsymbol{\alpha}_i^j \neq \boldsymbol{\beta}_i^j$. Differentiating equation (26) produces

$$\frac{\partial \mathbf{c}_i}{\partial x_l} = \frac{\partial \mathbf{F}^j}{\partial x_l}\boldsymbol{\beta}_i^j. \tag{27}$$

Rewriting equation (26) as $\boldsymbol{\beta}_i^j = (\mathbf{F}^j)^{-1}\mathbf{c}_i$, equation (27) becomes

$$\frac{\partial \mathbf{c}_i}{\partial x_l} = \frac{\partial \mathbf{F}^j}{\partial x_l}(\mathbf{F}^j)^{-1}\mathbf{c}_i.$$

The time derivative is approximated using a simple finite difference representation

$$\frac{\partial c_i}{\partial t} = \frac{1}{\Delta t}[c_i(t + \Delta t) - c_i(t)] = \frac{1}{\Delta t}(c_{i1} - c_{i0}),$$

where c_{i1} are the nodal values of c_i at time $t + \Delta t$ and c_{i0} are the values at time t. For the first time step, $c_{i0} = c_{i1} = c_i(t = 0)$.

In order to deal with the non-linear terms appearing in (15), a standard linear approximation can be used, where the approximated gradient of the concentration is written as the diagonal matrixes ($\mathbf{V}_l$) containing the values of the differential operators

$$\sum_{m=1}^{N} \mathbf{K}_m^j \frac{\partial \mathbf{c}_m}{\partial x_l}$$

for *a priori* estimation of the concentration at the interpolation nodal points at each time step; thus

$$\left(\sum_{m=1}^{N} \mathbf{K}_m^j \frac{\partial \mathbf{c}_m}{\partial x_l}\right)\frac{\partial \mathbf{c}_i}{\partial x_l} = \mathbf{V}_l^j \frac{\partial \mathbf{F}^j}{\partial x_l}(\mathbf{F}^j)^{-1}\mathbf{c}_i \quad (i = 1, \ldots, N, \quad j = 1, \ldots, M, \quad l = 1, 2),$$

where

$$\mathbf{V}_l^j = \left(\sum_{m=1}^{N} \mathbf{K}_m^j \frac{\partial \mathbf{c}_m}{\partial x_l}\right) \approx \frac{\partial \mathbf{F}_j}{\partial x_l}(\mathbf{F}^j)^{-1}\left(\sum_{m=1}^{N} \mathbf{K}_m^j \tilde{\mathbf{c}}_m\right).$$

The above expression for the non-linear terms makes the procedure iterative, since it is necessary to assume *a priori* estimation of the concentration at each time step, $\tilde{\mathbf{c}}(t_m + \Delta t) = \mathbf{c}(t_m)$, at the interpolation nodal points, in order to evaluate the concentration $\mathbf{c}(t_m + \Delta t)$ in the first iteration, using the corresponding boundary-only integral equation discussed before. Letting the evaluated $c(t_m + \Delta t)$ in the nth iteration become $\tilde{\mathbf{c}}(t_m + \Delta t)$ in the $(n + 1)$th iteration, the process is continued until convergence is obtained at each time step.

Now the non-homogeneous term $\mathbf{b}_i^j$ becomes

$$\mathbf{b}_i^j \approx (\mathbf{D}^j)^{-1}\left[\left[\mathbf{A}_i^j\left[-\sum_{l=1}^{2}\frac{\partial \mathbf{F}^j}{\partial x_l}(\mathbf{F}^j)^{-1}\left(\sum_{m=1}^{N}\mathbf{K}_m^j\tilde{\mathbf{c}}_m\right)\frac{\partial \mathbf{F}^j}{\partial x_l}(\mathbf{F}^j)^{-1}\mathbf{c}_i - \mathbf{P}_i^j + \mathbf{d}_i^j\mathbf{c}_i\right.\right.\right.$$
$$\left.+ n^j\frac{1}{\Delta t}(\mathbf{c}_{i1} - \mathbf{c}_{i0})\right] + \left\{\sum_{m=1}^{N}\mathbf{B}_m^j\left[\sum_{l=1}^{2}\frac{\partial \mathbf{F}^j}{\partial x_l}(\mathbf{F}^j)^{-1}\left(\sum_{k=1}^{N}\mathbf{K}_k^j\tilde{\mathbf{c}}_k\right)\frac{\partial \mathbf{F}^j}{\partial x_l}(\mathbf{F}^j)^{-1}\tilde{\mathbf{c}}_m\right.\right.$$
$$\left.\left.\left.+ \mathbf{P}_m^j - \mathbf{d}_m^j\tilde{\mathbf{c}}_m - n^j\frac{1}{\Delta t}(\tilde{\mathbf{c}}_{m1} - \tilde{\mathbf{c}}_{m0})\right]\right\}\mathbf{c}_i\right]\right],$$

where $\mathbf{D}^j$, $\mathbf{A}_i^j$ and $\mathbf{B}_m^j$ represent diagonal matrices containing terms

$$D^j = \prod_{p=1}^{N} D_p^j + \sum_{m=1}^{N}\left(K_m^j c_m \prod_{p=1}^{N}[D_p^j(1-\delta_{mp}) + \delta_{mp}]\right),$$

$$A_i^j = \prod_{p=1}^{N}[D_p^j(1-\delta_{pi}) + \delta_{pi}] + \sum_{m=1}^{N}\left((1-\delta_{mp})K_m^j c_m \prod_{p=1}^{N}\{[D_p^j(1-\delta_{ip}) + \delta_{ip}](1-\delta_{mp}) + \delta_{mp}\}\right)$$

and

$$B_m^j = (1-\delta_{mi})K_m^j \prod_{p=1}^{N}\{[D_p^j(1-\delta_{ip}) + \delta_{ip}](1-\delta_{mp}) + \delta_{mp}\}$$

respectively.

Defining

$$\mathbf{S}^j = (\mathbf{H}^j\hat{\mathbf{C}}^j - \mathbf{G}^j\hat{\mathbf{Q}}^j)(\mathbf{F}^j)^{-1}$$

and substituting the expression for $\mathbf{b}_i$, equation (25) becomes

$$\mathbf{H}^j\mathbf{c}_i - \mathbf{G}^j\mathbf{q}_i = \mathbf{S}^j(\mathbf{D}^j)^{-1}\left[\left[\mathbf{A}_i^j\left[-\sum_{l=1}^{2}\frac{\partial \mathbf{F}^j}{\partial x_l}(\mathbf{F}^j)^{-1}\left(\sum_{m=1}^{N}\mathbf{K}_m^j\tilde{\mathbf{c}}_m\right)\frac{\partial \mathbf{F}^j}{\partial x_l}(\mathbf{F}^j)^{-1} + \mathbf{d}_i^j\right]\right.\right.$$
$$+\left\{\sum_{m=1}^{N}\mathbf{B}_m^j\left[\sum_{l=1}^{2}\frac{\partial \mathbf{F}^j}{\partial x_l}(\mathbf{F}^j)^{-1}\left(\sum_{k=1}^{N}\mathbf{K}_k^j\tilde{\mathbf{c}}_k\right)\frac{\partial \mathbf{F}^j}{\partial x_l}(\mathbf{F}^j)^{-1}\tilde{\mathbf{c}}_m + \mathbf{P}_m^j - \mathbf{d}_m^j\tilde{\mathbf{c}}_m\right.\right.$$
$$\left.\left.\left.-\frac{n^j}{\Delta t}(\tilde{\mathbf{c}}_{m1} - \tilde{\mathbf{c}}_{m0})\right]\right\}\right]\mathbf{c}_i - \mathbf{S}^j(\mathbf{D}^j)^{-1}\mathbf{A}_i^j\mathbf{P}_i^j + \frac{n^j}{\Delta t}\mathbf{S}^j(\mathbf{D}^j)^{-1}\mathbf{A}_i^j(\mathbf{c}_{i1} - \mathbf{c}_{i0})$$
$$(i = 1, \ldots, N, \quad j = 1, \ldots, M).$$

Defining the new matrix

$$\mathbf{T}^j = \mathbf{S}^j(\mathbf{D}^j)^{-1}\left[\left[\mathbf{A}_i^j\left[-\sum_{l=1}^{2}\frac{\partial \mathbf{F}^j}{\partial x_l}(\mathbf{F}^j)^{-1}\left(\sum_{m=1}^{N}\mathbf{K}_m^j\tilde{\mathbf{c}}_m\right)\frac{\partial \mathbf{F}^j}{\partial x_l}(\mathbf{F}^j)^{-1} + \mathbf{d}_i^j\right]\right.\right.$$
$$\left.\left.-\left\{\sum_{m=1}^{N}\mathbf{B}_m^j\left[-\sum_{l=1}^{2}\frac{\partial \mathbf{F}^j}{\partial x_l}(\mathbf{F}^j)^{-1}\left(\sum_{k=1}^{N}\mathbf{K}_k^j\tilde{\mathbf{c}}_k\right)\frac{\partial \mathbf{F}^j}{\partial x_l}(\mathbf{F}^j)^{-1}\tilde{\mathbf{c}}_m - \mathbf{P}_m^j + \mathbf{d}_m^j\tilde{\mathbf{c}}_m + \frac{n^j}{\Delta t}(\tilde{\mathbf{c}}_{m1} - \tilde{\mathbf{c}}_{m0})\right]\right\}\right],$$

the following expression is obtained:

$$\mathbf{H}^j\mathbf{c}_i - \mathbf{G}^j\mathbf{q}_i = \mathbf{T}^j\mathbf{c}_i + \frac{n^j}{\Delta t}\mathbf{S}^j(\mathbf{D}^j)^{-1}\mathbf{A}_i^j(\mathbf{c}_{i1} - \mathbf{c}_{i0}) - \mathbf{S}^j(\mathbf{D}^j)^{-1}\mathbf{A}_i^j\mathbf{P}_i^j. \tag{28}$$

A linear variation of c_i and q_i within each time step may now be defined, i.e.

$$c_i = (1-\theta_c)c_{i0} + \theta_c c_{i1}, \qquad q_i = (1-\theta_q)q_{i0} + \theta_q q_{i1},$$

where θ_c and θ_q take values between zero and unity. After this time step scheme has been applied, equation (28) becomes

$$\left((\mathbf{H}^j - \mathbf{T}^j)\theta_c - \frac{n^j}{\Delta t}\mathbf{S}^j(\mathbf{D}^j)^{-1}\mathbf{A}_i^j\right)\mathbf{c}_{i1} - \mathbf{G}^j\theta_q\mathbf{q}_{i1}$$
$$= \left((\mathbf{T}^j - \mathbf{H}^j)(1-\theta_c) - \frac{n^j}{\Delta t}\mathbf{S}^j(\mathbf{D}^j)^{-1}\mathbf{A}_i^j\right)\mathbf{c}_{i0} - \mathbf{G}^j(1-\theta_q)\mathbf{q}_{i0} - \mathbf{S}^j(\mathbf{D}^j)^{-1}\mathbf{A}_i^j\mathbf{P}_i^j.$$

Using the same linear approximation at each iteration as before, the matching conditions on the interface of the layers, equation (8), take the form

$$\left\{-(D_i^m + \tilde{c}_i^m K_i^m)\frac{\partial c_i^m}{\partial n} - \tilde{c}_i^m \sum_{k=1}^{N}\left[\left(K_k^m \frac{\partial \tilde{c}_k^m}{\partial n}\right)(1-\delta_{ik})\right]\right\}\Bigg|_m$$
$$= \left\{-(D_i^{m+1} + \tilde{c}_i^{m+1}K_i^{m+1})\frac{\partial c_i^{m+1}}{\partial n} - \tilde{c}_i^{m+1}\sum_{k=1}^{N}\left[\left(K_k^{m+1}\frac{\partial \tilde{c}_k^{m+1}}{\partial n}\right)(1-\delta_{ik})\right]\right\}\Bigg|_m$$
$$(i = 1, \ldots, N, \quad m = 1, \ldots, M-1).$$

4. NUMERICAL EXAMPLES

To validate the numerical model given in Section 3, a few numerical examples are presented for the cases of a single gas and a binary mixture, in all the numerical examples the values of θ_c and θ_q were chosen to be 0·5 and 1, respectively. In the first example of a single gas a homogeneous isotropic porous medium with 10 m × 10 m vertical cross-section was taken as a model domain with porosity $n = 50\%$, diffusion coefficient $D = 1{\cdot}0\ \text{m}^2\ \text{day}^{-1}$, reaction constant $d = 0{\cdot}0\ \text{s}^{-1}$, source term $P = 0{\cdot}005\ \text{kg m}^{-3}\ \text{day}^{-1}$ and $K = 1$, 10 and 100 $\text{m}^5\ \text{kg}^{-1}\ \text{day}^{-1}$. The geometry of the model domain, boundary conditions and locations of internal points for each case study are shown in Figure 2. These locations were chosen through numerical experiments, so the best convergence was obtained. As can be observed, the number and location of internal points depend on the problem parameters. It is possible to increase the accuracy of the solution by increasing the number of internal points, but this incurs a heavy computing time penalty.

It is important to note that the matrix **F** is non-singular if the nodal points are all distinct; however, when using a large number of internal points, the condition number of the matrix **F** becomes very large and therefore the matrix **F** behaves numerically as singular. Recently Powell[12] has developed an efficient stable algorithm to solve this inversion problem when the number of nodal points is large; here we have used only standard Gauss elimination with pivoting, restricting ourselves to not too large number of internal points.

Figures 3(a)–3(c) show the concentration profiles for different times and different values of K. In each case the initial concentration of gas was taken to be equal to zero, $C_0 = 0$, with zero-flux boundary condition through the bottom and at the two sides of the model domain.

Comparison of the steady state condition obtained after simulation for a long enough period of time and the steady state analytical solution (33) given in the Appendix (to our knowledge these analytical solutions have not been reported previously in the open literature) is shown in Figure 4(a) for different values of K. It can be observed that the model shows good agreement with the analytical solution.

The time variation of the flux through the upper boundary obtained and the asymptotic value evaluated from (35) are shown in Figure 4(b) for different values of K. The model is in good agreement with the analytical solution for the flux, showing that the mass balance is preserved.

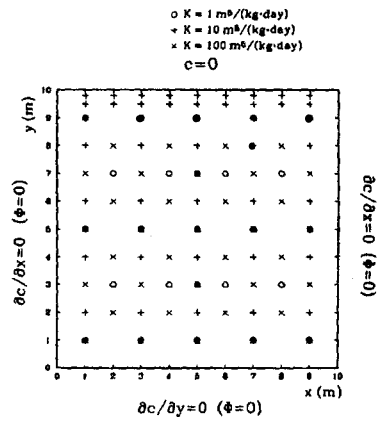

Figure 2. Geometry of model domain, boundary conditions and locations of internal points

It can be noted that the maximum error in flux at the free surface increases when K increases, being equal to 5·5 per cent for $K = 100$ m^5 kg^{-1} day^{-1}.

When the same numerical example was performed for $K = 100$ m^5 kg^{-1} day^{-1} with a different value for the boundary condition at the free surface, $C_0 = 0{\cdot}7$ kg m^{-3} instead of zero, an unexpected error of 32 per cent for the flux through the free surface was found (see Figure 5).

It is important to point out that in both cases, with and without zero concentration at the free surface, the steady state flux through the free surface has to be the same, since the two cases have the same source term. In the case of $C_0 = 0$ the flux through the free surface is given by $D(\partial C/\partial n)$ with $D = 1$ m^2 day^{-1}, but in the case of $C_0 = 0{\cdot}7$ kg m^{-3} the flux is given by $(D + KC_0)(\partial C/\partial n)$ with $K = 100$ m^5 kg^{-1} day^{-1} and $D = 1$ m^2 day^{-1}. Therefore the magnitude of the normal derivative in the case of non-zero boundary condition has to be two orders of magnitude smaller than in the other case. This difference appears to be the reason for the discrepancy found in the estimation of the flux in the case of non-zero boundary condition at the free surface.

To overcome this difficulty, a technique commonly employed in laboratory studies, but not in numerical analysis, is used. By scaling the flow domain, as is usually done on a physical model, it is possible to obtain a concentration profile with a larger gradient, since ∇C has the dimension of (mass)/(length)^4. To ensure complete physical similarity between the original problem and the scaled one, we must change the parameters of the model according to the scaling factor; in this way the parameters D and K decrease in the scale model, since they are of the order of (length)^2/(time) and (length)^5/(mass × time) respectively. One of the major difficulties in implementing a physical model is that sometimes the magnitude of one variable or parameter of the model becomes impossible to obtain in a laboratory experiment, requiring a distorted model. This problem does not present itself in a numerical model, because there is no physical limitations on predicting the magnitude of a quantity, as long as it is consistent with the scaling factor to ensure physical similarity. This is the case of the present example, where the concentration increases with the scaling factor, reaching values greater than unity, since the concentration has the dimension of (mass)/(length)^3. In this way, as the scaling factor (unit length (UL)) increases, the concentration and its derivative approach the same order of magnitude (see Table I). Table I and Figure 5 show how the accuracy of the flux is improved by the scaling process.

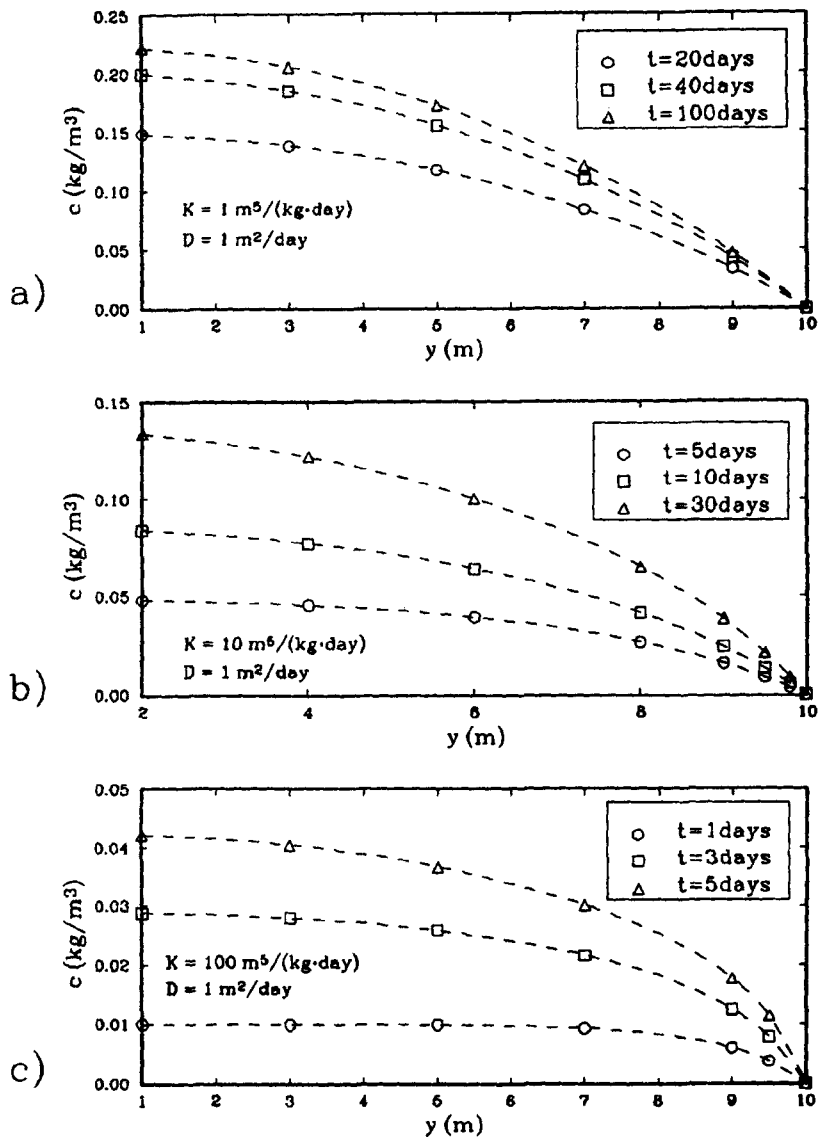

Figure 3. Concentration profiles for different times and different values of K

The next two numerical examples, each with a different boundary condition at the free surface ($C_0 = 0$ and 0·7 kg m^{-3}), were carried out for a rectangular repository of width 6 m, consisting of three layers of heights $l^1 = l^2 = 5$ and $l^3 = 2$ m, with values of the parameter K at each layer of $K^1 = 1000$, $K^2 = 1200$ and $K^3 = 100$ m^5 kg^{-1} day^{-1}, production terms $P^1 = 0{\cdot}003$, $P^2 = 0{\cdot}005$ and $P^3 = 0$ kg m^{-3} day^{-1}, diffusion coefficients $D^1 = D^2 = D^3 = 1{\cdot}5$ m^2 day^{-1} and zero reaction constant.

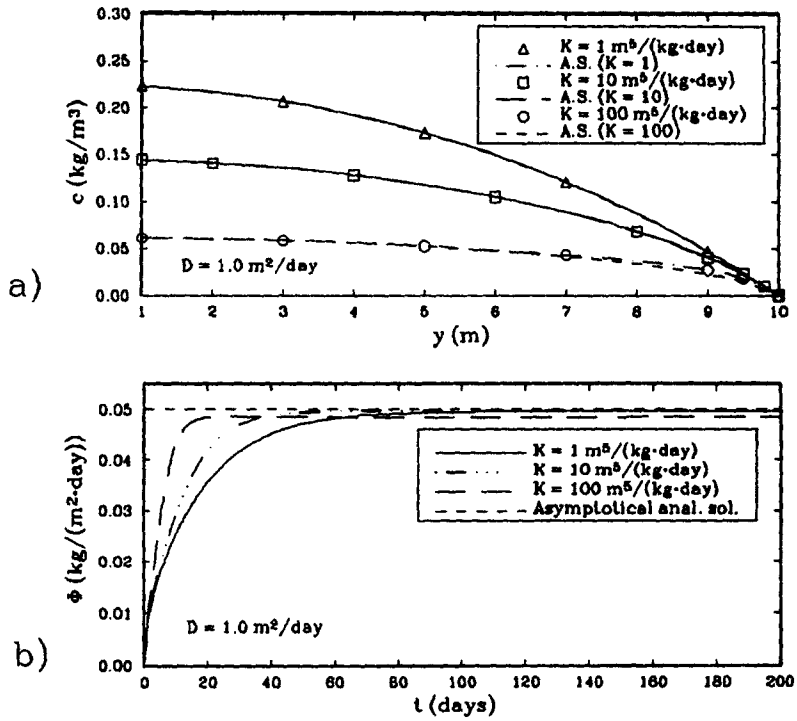

Figure 4. (a) Comparison of concentration profiles with analytical solution (A.S.) for different K. (b) Change in flux on upper boundary and asymptotic solution for different K

Similar difficulties to those found for the case of the one-layer domain with surface concentration different from zero were encountered when dealing with the multilayer problem even in the case of $C_0 = 0$ kg m^{-3}, because the concentration at each interface is different from zero and hence for large values of K the estimation of the flux-matching condition will depend strongly on the accuracy of the normal derivative at each interface. In the present numerical examples a scaling factor of 1/1000, i.e. unit length (UL) of 1000 m, was used.

Figures 6(a) and 6(b) show the concentration profiles for the case of $C_0 = 0$ kg m^{-3} during the transient process and at the steady state respectively, while Figure 6(c) shows the change in flux with time through each interface and at the free surface. In these figures the concentration profile and flux at the steady state are compared with the analytical solution given in the Appendix, showing good agreement.

The maximal error in the concentration profile was about 4 per cent and the flux error through the first interface ($y = 5$ m) was 0·20 per cent, through the second interface ($y = 10$ m) 1·15 per cent and through the free surface ($y = 12$ m) 8·79 per cent, which is to be expected owing to the boundary layer effect at the free surface.

It can also be noticed that the gas flows from the second layer into the first and third layers in the first period, since $P^2 = 0{\cdot}005 > P^1 = 0{\cdot}003 > P^3 = 0$ kg m^{-3} day^{-1}, but after some time, when the concentration in the first layer has increased sufficiently, the gas starts to flow from the first to the second layer and from the second to the third layer.

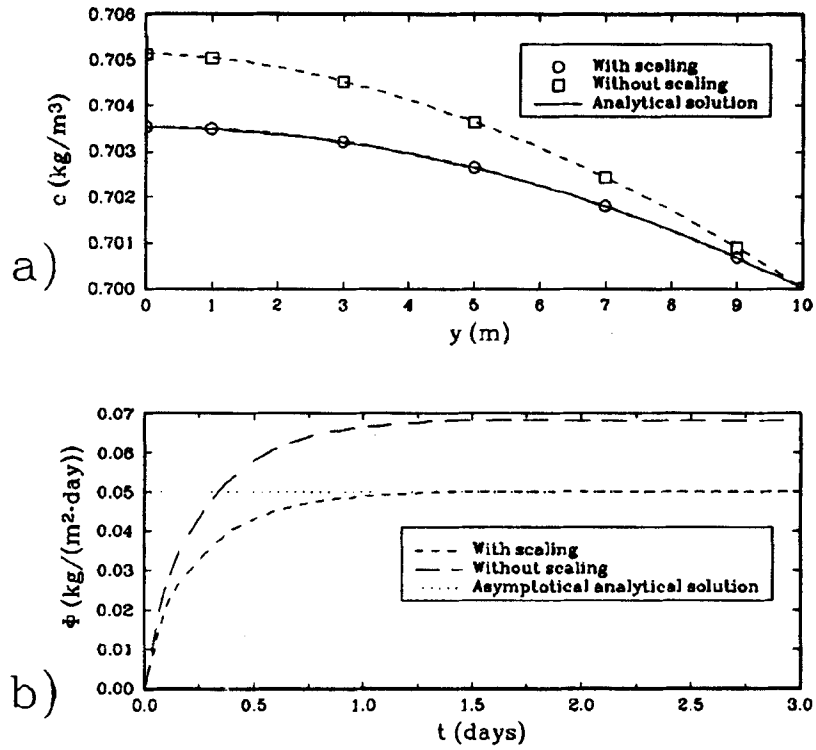

Figure 5. Comparison of accuracy of results with analytical solution without and with scaling for (a) concentration and (b) flux

Figures 7(a)–7(c) are equivalent to Figures 6(a)–6(c) but for the case of non-zero boundary condition at the free surface, $C_0 = 0{\cdot}7$ kg mg^{-3}. In this case more accurate results were obtained than in the previous case, because the boundary layer effect is much smaller. The maximum error obtained was $2{\cdot}85 \times 10^{-4}$ per cent for the concentration and 0·17 per cent for $\Phi(L^1)$, 0·13 per cent for $\Phi(L^2)$ and 0·12 per cent for $\Phi(L^3)$. It is important to point out that this case is one with physical meaning corresponding to the case of the flux of the mixture of gases.

For the case of two gases, binary flow, we will first consider rectangular domain of 10×10 m^2, consisting of two layers of heights $l^1 = 7$ and $l^2 = 3$ m.

The parameters K_i^j and D_i^j are assumed to be the same for both gases but different in each layer, so the obtained numerical results can be compared with the developed analytical solutions (see Appendix). Values of the parameters are $K_1^1 = K_2^1 = 10$ and $K_1^2 = K_2^2 = 3$ m^5 kg^{-1} day^{-1} and $D_1^1 = D_2^1 = D_1^2 = 2$ m^2 day^{-1}. The decay term d_i^j is assumed to be zero for both gases.

Table I. Improvement in accuracy of model by scaling

UL	C_0 (kg m^{-3})	$(\partial c/\partial n)_{\text{theor}}$ (kg m^{-2} day^{-1})	$(\partial c/\partial n)_{\text{numer}}$ (kg m^{-2} day^{-1})	$\lvert\Delta\Phi/\Phi\rvert$ (%)
10^0	7×10^{-1}	$7{\cdot}04 \times 10^{-4}$	$9{\cdot}3 \times 10^{-4}$	32
10^1	7×10^2	$7{\cdot}04 \times 10^0$	$7{\cdot}78 \times 10^0$	10·5
10^2	7×10^5	$7{\cdot}04 \times 10^4$	$7{\cdot}06 \times 10^4$	0·26

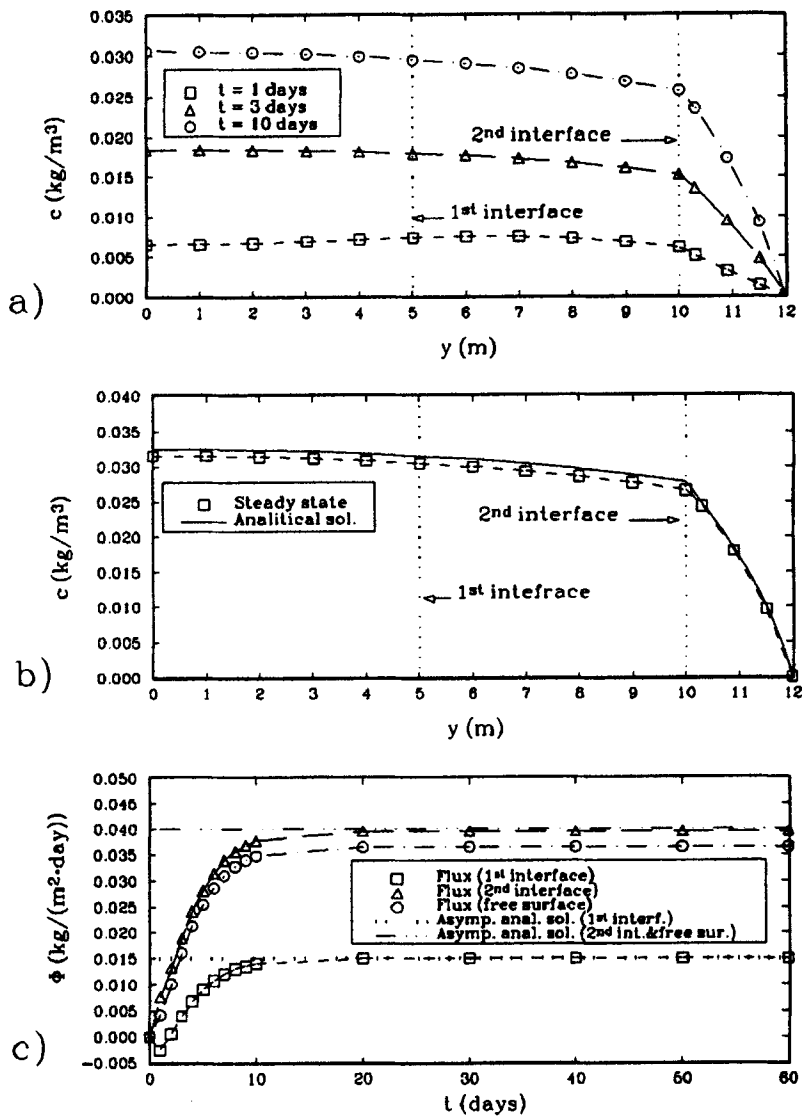

Figure 6. (a) Change in concentration profile with time. (b) Steady state concentration profile. (c) Change in flux with time. $C_0 = 0$ kg m^{-3}

The initial concentrations are taken to be $c_1(x, y, 0) = 0{\cdot}0$ and $c_2(x, y, 0) = 0{\cdot}7$ kg m^{-3} and the boundary conditions at the free surface are $c_1(x, (l^1 + l^2), t) = c_0 = 0{\cdot}0$ and $c_2(x, (l^1 + l^2), t) = 0{\cdot}7$ kg m^{-3}. All production terms are zero, except $P_1^1 = 0{\cdot}005$ kg m^{-3} day^{-1}.

Figures 8(a)–8(b) show the concentration profiles during the transient process and at the final steady state for each gas respectively. Figure 8(c) shows the change in flux with time through the interface between the two layers and at the free surface for each gas. This figure also presents the asymptotic condition corresponding to the case where the gas emission to the atmosphere is equal to the total production. As expected, the flux of the first gas through the interface increases faster than the flux through the free surface, since this gas for $t = 0$ is not present in the domain and has

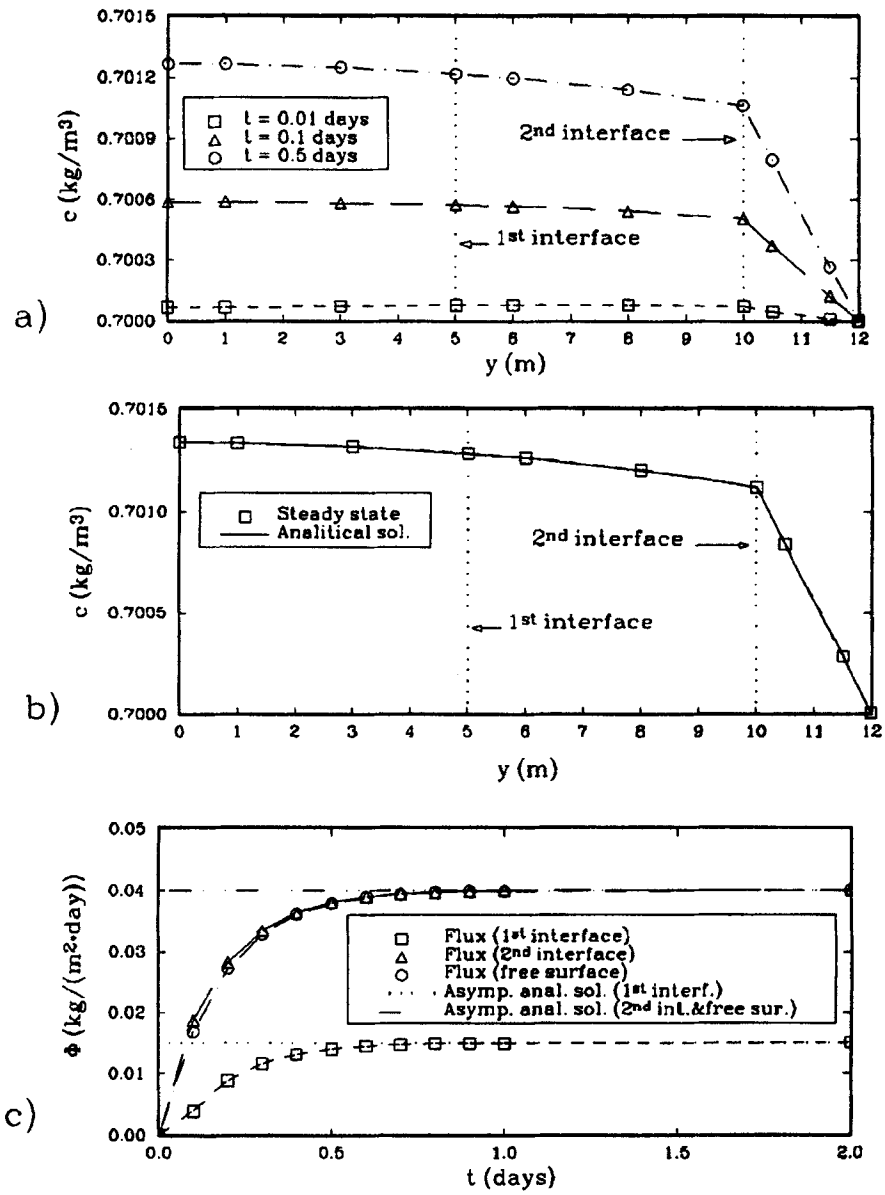

Figure 7. (a) Change in concentration profile with time. (b) Steady state concentration profile. (c) Change in flux with time. $C_0 = 0{\cdot}7$ kg m^{-3}

production only in the first layer. The flux of the second gas through the interface increases slower than the flux through the free surface, since this gas is present inside the domain for $t = 0$, has no production in both layers and there is flux of both gases from the first layer into the second layer.

In the second numerical example, with higher values of the constants K_i^j, a rectangular domain of 1×1 m^2 was considered, consisting of two layers of heights $l^1 = 0{\cdot}8$ and $l^2 = 0{\cdot}2$ m. In this case, since the values of K_i^j are much higher than in the previous example, i.e. $K_1^1 = K_2^1 = 100$ and

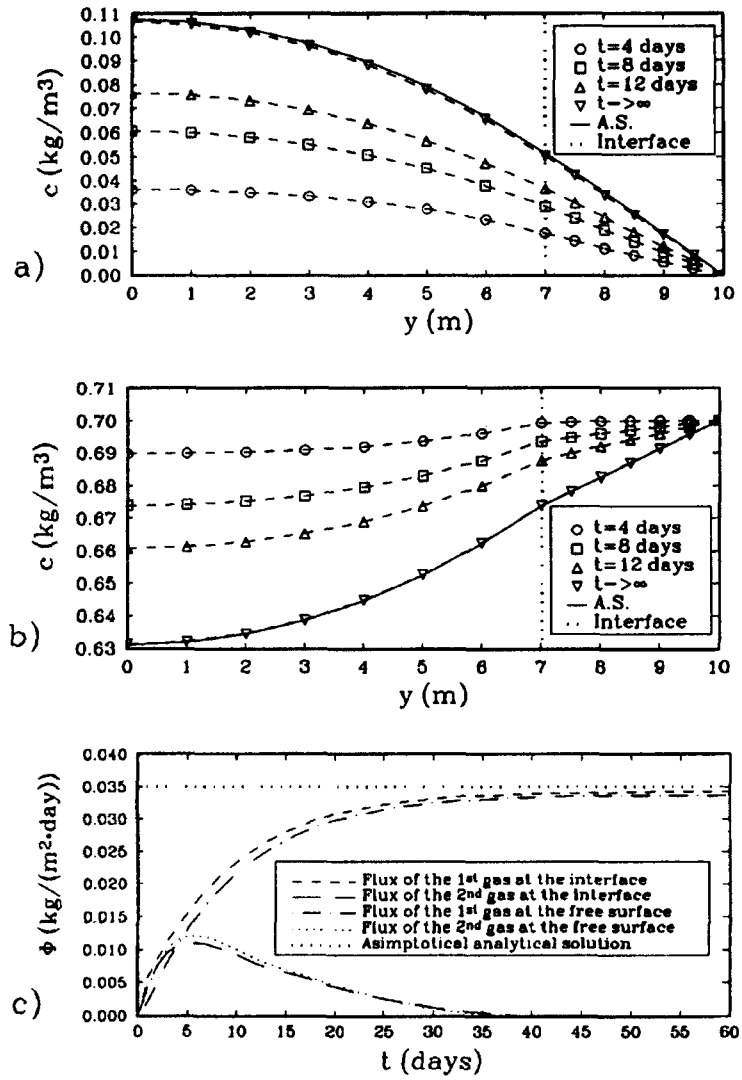

Figure 8. Concentration profiles (a) during transient process and (b) at final steady state for each gas. (c) Change in flux with time at interface between two layers and at free surface for each gas

$K_1^2 = K_2^2 = 10$ m^5 kg^{-1} day^{-1}, a much higher density of internal points is needed in order to achieve the required accuracy of results, which makes this estimation more expensive in terms of computer time. The small porous domain was chosen in this case in order to achieve the requirement of a higher density of internal points with only a few of them. Here the constants D_i^j were taken as $D_1^1 = D_2^1 = D_1^2 = D_2^2 = 1$ m^2 day^{-1}, while production terms and initial and boundary conditions were the same as in the previous numerical example.

Figures 9(a) and 9(b) show the concentration profiles during the transient process and at the final steady state compared with the analytical solution for each gas respectively. In Figure 9(c) the changes in flux through the free surface for the first and second gases are presented, as well as the change in total flux as the sum of the two fluxes. It can be observed that the total flux curve behaves

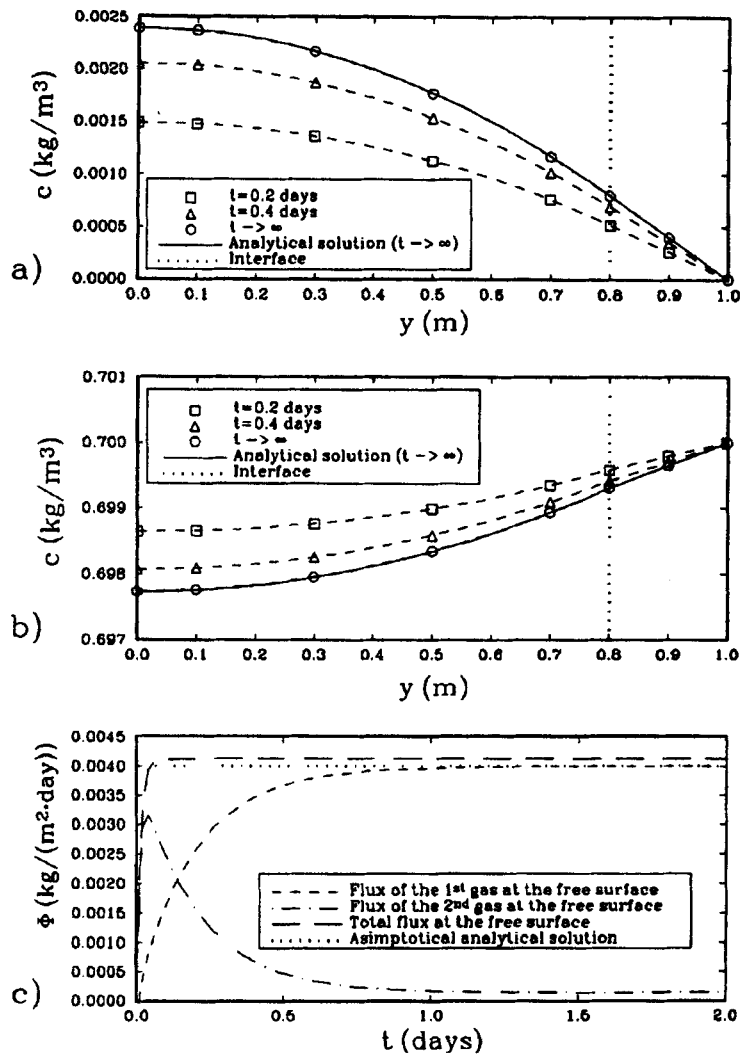

Figure 9. Concentration profiles (a) during transient process and (b) at final steady state compared with analytical solution for both gases. (c) Change in flux with time at free surface for each gas

as a step function for high values of K_i^j, reaching the steady state constant value in a very short time, while its components are still changing. It is known that such a behaviour is very difficult to predict and usually in numerical models it causes oscillatory behaviour, which is not present here.

5. CONCLUSIONS

From the comparison between the obtained numerical results and the corresponding analytical solutions we can conclude that the proposed numerical technique is a reasonable and simple one, consisting only of boundary integrals, for the solution of the problem of flux of a multicomponent mixture of gases out of a multilayer landfill.

As was pointed out before, the main advantage of this kind of boundary-only formulation in relation to domain methods is the reduction in data preparation, since only surface elements are necessary. From the mathematical point of view the present numerical model tested here for two gases in a three-layer landfill of rectangular shape can be implemented for the general case of a repository of arbitrary shape consisting of n layers and m gases, only requiring more computer capacity.

A numerical model such as the one presented here, which can simulate the migration of gases through a landfill and their release into the atmosphere, can be used as an efficient tool for the evaluation of possible control structures to minimize the release of such gases, as well as a way to estimate and predict the amount of gases released.

ACKNOWLEDGEMENT

This work was performed under the auspices of the ISC Programme of the European Commission, contract CI1*-CT94-0077VE.

APPENDIX: ANALYTICAL SOLUTIONS

In general, equation (1) cannot be solved analytically, but with some simplifications the analytical solution for the time-independent form of (1) can be obtained (steady state).

Let us first consider the 1D case of a single gas in a multilayer domain with constant coefficients D^j and K^j in each layer and reaction coefficients d^j equal to zero. Under these conditions, equation (1) becomes

$$D^j \frac{\mathrm{d}^2 c}{\mathrm{d}y^2} + K^j \frac{\mathrm{d}}{\mathrm{d}y}\left(c \frac{\mathrm{d}c}{\mathrm{d}y}\right) + P^j = 0 \quad (j = 1, \ldots, M), \tag{29}$$

with boundary conditions (see Figure 10)

$$\frac{\mathrm{d}c}{\mathrm{d}y} = 0 \quad \text{at} \quad y = 0, \qquad c = C_0 \quad \text{at} \quad y = L^M \tag{30}$$

and matching conditions

$$(D^m + K^m c)\frac{\mathrm{d}c}{\mathrm{d}y}\bigg|_m = (D^{m+1} + K^{m+1} c)\frac{\mathrm{d}c}{\mathrm{d}y}\bigg|_m \quad (m = 1, \ldots, M-1), \tag{31}$$

$$c^m|_m = c^{m+1}|_m. \tag{32}$$

Integrating equation (29) twice and using the boundary and matching conditions, we obtain

$$c(y) = -\frac{D^j}{K^j} + \sqrt{\left[\left(\frac{D^j}{K^j}\right)^2 - \frac{2}{K^j}\left(\tfrac{1}{2} P^j y^2 + A^j y + B^j\right)\right]}, \quad y \in [L^{j-1}, L^j], \tag{33}$$

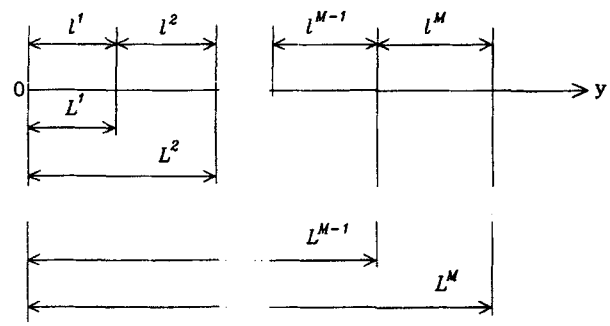

Figure 10. 1D model domain for analytical solution

where

$$A^1 = 0, \qquad A^j = \sum_{m=1}^{j-1} [(P^m - P^{m+1})L^m] \quad (j = 2, \ldots, M), \tag{34}$$

$$B^j = \frac{(D^j)^2}{2K^j} - \tfrac{1}{2}P^j(L^j)^2 - L^jA^j - \frac{K^j}{2}\left\{\frac{D^j}{K^j} - \frac{D^{j+1}}{K^{j+1}} + \sqrt{\left[\left(\frac{D^{j+1}}{K^{j+1}}\right)^2 - \frac{2}{K^{j+1}}(\tfrac{1}{2}P^{j+1}(L^j)^2 + A^{j+1}L^j + B^{j+1})\right]}\right\}^2 \quad (j = 1, \ldots, M-1)$$

$$B^M = -\left(D^M C_0 + \frac{K^M}{2}C_0^2 + \tfrac{1}{2}P^M(L^M)^2 + A^M L^M\right),$$

with

$$L^m = \sum_{k=1}^{m} l^k, \qquad L^0 = 0$$

and l^k the thickness of the kth layer (see Figure 10).

Finally the expression for the flux is given as

$$\Phi^j(y) = -(D^j + K^j c)\frac{\mathrm{d}c}{\mathrm{d}y} = A^j + P^j y, \quad y \in (L^{j-1}, L^j]. \tag{35}$$

In the case of two gases the analytical solution can be found if we consider the same simplifications as before, with the addition that the constants have to be the same for both gases in each layer. The main difference between this case and the previous one is that now the production term, initial and boundary conditions for each gas are different. Using these simplifications, equation (1) becomes

$$D^j\frac{\mathrm{d}^2 c_i}{\mathrm{d}y^2} + K^j\frac{\mathrm{d}}{\mathrm{d}y}\left(c_i\frac{\mathrm{d}c}{\mathrm{d}y}\right) + P_i^j = 0 \quad (i = 1, 2, \quad j = 1, \ldots, M), \tag{36}$$

where $c = c_1 + c_2$, with boundary conditions (see Figure 10)

$$\frac{\mathrm{d}c_i}{\mathrm{d}y} = 0 \quad \text{at} \quad y = 0 \quad (i = 1, 2), \tag{37}$$

$$c_i = 0 \quad \text{or} \quad c_i = C_{i0} \quad \text{at} \quad y = L^M \tag{38}$$

and matching conditions

$$\left(D^m \frac{dc_i}{dy} + K^m c_i \frac{dc}{dy}\right)\Big|_m = \left(D^{m+1} \frac{dc_i}{dy} + K^{m+1} c_i \frac{dc}{dy}\right)\Big|_m,$$
$$c_i^m|_m = c_i^{m+1}|_m \quad (i = 1, 2, \quad m = 1, \ldots, M-1).$$

As was shown in Section 2, if we add the equations for $i = 1$ and 2, the total emission of the two gases can be determined using the single-gas analytical solution.

If we assume that one of the gases, e.g. $i = 1$, has no production term, i.e. $P_1^j = 0$, which is true in the case of landfills, corresponding to the simulation of the air inside the repository, then the following equation for $c_1(y)$ is obtained:

$$c_1(y) = C_{10} \exp\left(-\frac{K^j}{D^j}[c(y) - c(L^j)] - \sum_{l=j+1}^{M} \frac{K^l}{D^l}[c(L^{l-1}) - c(L^l)]\right), \quad y \in [L^{j-1}, L^j]. \tag{39}$$

The solution for the second gas is obtained from the relation

$$c_2(y) = c(y) - c_1(y), \tag{40}$$

where the total concentration c is found from (33).

The following expressions for the fluxes of the first and second gases are obtained:

$$\Phi_1^j = -D^j \frac{dc_1}{dy} - c_1\left(K^j \frac{dc_1}{dy} + K^j \frac{dc_2}{dy}\right) = 0 \quad (j = 1, \ldots, M), \tag{41}$$

$$\Phi_2^j = -D^j \frac{dc_2}{dy} - c_2\left(K^j \frac{dc_1}{dy} + K^j \frac{dc_2}{dy}\right) = P_2^j y + A_2^j \quad (j = 1, \ldots, M), \tag{42}$$

where A_2^j is given by (34) as

$$A_2^1 = 0, \qquad A_2^j = \sum_{m=1}^{j-1} [(P_2^m - P_2^{m+1})L^m] \quad (j = 2, \ldots, M).$$

REFERENCES

1. J. T. Houghton, B. A. Callander and S. K. Varney (eds), *Climate Change 1992. Supplementary Report to the IPCC Scientific Assessment*, published for the Environmental Panel on Climate Change, Cambridge University Press, Cambridge, 1992.
2. R. E. Dickenson and R. J. Cicerone, 'Future global warming from atmospheric trace gases', *Nature*, **319**, 109–115 (1986).
3. V. Ramanathan *et al.* 'Climate–chemical interaction and the effects of changing atmospheric trace gases', *J. Geophys. Res.*, **25**, 1441–1482 (1987).
4. R. Lassey, D. Lowe, M. Manning and G. Waghorn, 'A source inventory for atmospheric methane in New Zealand and its global perspective', *J. Geophys. Res.: Atmos.*, (1991).
5. C. A. Brebbia and J. Dominguez, *Boundary Elements—An Introductory Course*, Computational Mechanics Publications, Southampton/McGraw-Hill, New York, 1989.
6. A. N. Findikakis and J. O. Leckie, 'Numerical simulation of gas flow in sanitary landfills', *J. Environ. Eng. Div., Proc. Am. Soc. Civil Eng.*, **105**, (1979).
7. F. R. Troeh, J. D. Jabro and D. Kirkham, 'Gaseous diffusion equations for porous materials', *Geoderma*, **27**, 239–253 (1982).
8. R. E. Cunningham and R. J. J. Williams, *Diffusion in Gases and Porous Media*, Plenum, New York, 1980.
9. D. Nardini and C. A. Brebbia, 'A new approach to free vibration analysis using boundary elements', in *Boundary Element Methods in Engineering*, Computational Mechanics Publications, Southampton/Springer, Berlin, 1982.
10. S. Ahmad and P. K. Banerjee, 'A new method in vibration analysis by BEM using particular integrals', *J. Eng. Mech. Div. ASCE*, **113**, 682–695 (1986).
11. C. A. Michelli, 'Interpolations of scattered data', *Distance Matrices and Conditionally Positive Definite Functions—Const. Approx.*, **2** (1986).
12. M. J. D. Powell, 'Some algorithms for thin plate spline interpolation to functions of two variables', *University of Cambridge Numerical Analysis Rep. NA6*, 1993.